Results in Physics 6 (2016) 107–111

Contents lists available at ScienceDirect

Results in Physics

journal homepage: www.journals.elsevier.com/results-in-physics

Effect of wavelength on the electrical parameters of a vertical parallel junction silicon solar cell illuminated by its rear side in frequency domain

Gökhan Sahin *

Electric and Electronic Engineering Department, IĞDIR University, Iğdır 76000, Turkey

ARTICLE INFO

Article history:
Received 21 January 2016
Accepted 17 February 2016
Available online 2 March 2016

Keywords:
Vertical parallel junction
Wavelength
Frequency modulation
Electrical parameters

ABSTRACT

The influence of the illumination wavelength on the electrical parameters of a vertical parallel junction silicon solar cell by its rear side is theoretically analyzed. Based on the excess minority carrier's density, the photocurrent density and photovoltage across the junction were determined. From both photocurrent and the photovoltage, the series and shunt resistance expressions are deduced and the solar cell associated capacitance and conversion efficiency are calculated.

The aim of this study is to show the influence of the illumination wavelength on the electrical parameters of the cell and the behavior of both parasitic resistances and capacitance versus operating point.

Introduction

The knowledge of both microscopic and electrical parameters of solar cell is of great importance in order to improve solar cell fabrication process and materials, leading to the higher conversion efficiency. Various techniques [1,2] have been developed for that purpose; particularly, previous work done by [3,4] have shown that the behavior of silicon solar cells is dependent on the illumination wavelength. The purpose of this paper is to investigate the influence of monochromatic illumination wavelength on the electrical parameters of a vertical junction polycrystalline silicon solar cell.

Theory

Fig. 1 represents parallel vertical junction solar cells under monochromatic light, in one dimensional model (Ox), where the studied p-base1 interacts with the two adjacent emitters.

We present on Fig. 2 a unit cell of a vertical junction's silicon solar cell under various wavelengths. H is the base width, θ is the illumination incidence angle and x is the depth in the base.

Given that the contribution of the base to the photocurrent is larger than that of the emitter [5] our analysis will only be developed in the base region (see Figs. 2 and 3).

Taking into account the generation, recombination and diffusion phenomena in the base, the equation governing the variation of the minority carrier's density $\delta(x,y,z,t)$ under modulation frequency [6–8] is:

$$D(\omega)\cdot\frac{\partial^2\delta(x,\theta,t)}{\partial x^2}-\frac{\delta(x,\theta,t)}{\tau}=-G(z,\theta,t)+\frac{\partial\delta(x,\theta,t)}{\partial t} \quad (1)$$

$D(\omega)$ [9] and τ are respectively, the excess minority carrier diffusion constant and lifetime.

The excess minority carriers' density can be written as:

$$\delta(x,t)=\delta(x)\exp(-j\omega t) \quad (2)$$

Carrier generation rate $G(z,\theta,t)$ is given by:

$$G(z,\theta,\lambda,t)=g(z,\theta,\lambda)\exp(-j\omega t) \quad (3)$$

where

$$g(z,\theta,\lambda)=\alpha(\lambda)(1-R(\lambda))\cdot\phi(\lambda)\cdot\exp(-\alpha(\lambda)\cdot z)\cdot\cos(\theta) \quad (4)$$

x is the base depth along x axis, ω is the angular frequency, θ is the incidence angle, z the base depth according to the vertical axis; Sf is the junction recombination velocity and λ the illumination wavelength.

If we replace Eq. (2) with Eq. (1), the temporary part is eliminated and we obtain:

$$\frac{\partial^2\delta(x)}{\partial x^2}-\frac{\delta(x,\theta,t)}{L(\omega)^2}=-\frac{g(z,\theta)}{D(\omega)} \quad (5)$$

* Tel.: +90 5535764285.
E-mail address: g.sahin38@hotmail.fr

http://dx.doi.org/10.1016/j.rinp.2016.02.003
2211-3797/

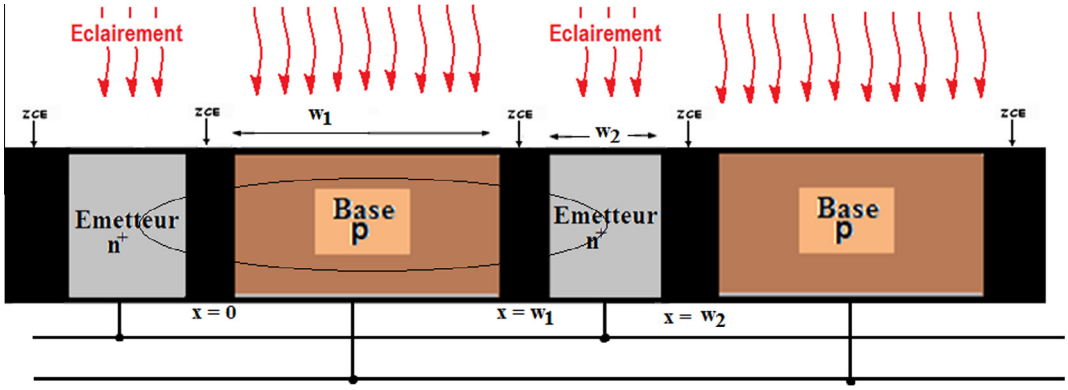

Fig. 1. Vertical parallel junction silicon solar cell.

The solution of this equation is:

$$\delta(x,\omega,\theta,z,Sf,\lambda) = A\cosh\left(\frac{x}{L(\omega)}\right) + B\sinh\left(\frac{x}{L(\omega)}\right) + \frac{L(\omega)^2}{D(\omega)} \cdot \alpha(\lambda)(1-R(\lambda)) \cdot \phi(\lambda) \cdot \exp(\alpha(\lambda)\cdot z) \cdot \cos(\theta) \quad (6)$$

Coefficients A and B are determined through the following boundary conditions [10]:

- at the junction ($x = 0$):

$$D(\omega)\cdot\left.\frac{\partial\delta(x,\omega,\theta)}{\partial x}\right|_{x=0} = Sf\cdot\delta(x,\omega,\theta)|_{x=0} \quad (7)$$

Sf is the excess minority carrier's recombination velocity at each junction [11].

- at the middle of the base ($x = H/2$) [12]:

$$D(\omega)\cdot\left.\frac{\partial\delta(x,\omega,\theta)}{\partial x}\right|_{x=\frac{H}{2}} = 0 \quad (8)$$

The excess minority carriers in the base will flow to the two junctions by diffusion; the photocurrent density is given by the following expression:

$$J_{Ph} = 2\cdot q\cdot D(\omega)\cdot\left.\frac{\partial\delta(x,\omega,\theta)}{\partial x}\right|_{x=0} \quad (9)$$

where q is the elementary charge.

Based on the excess minority carrier's density, we can determine the photovoltage across the junction, according to the Boltzmann relation, as inutile. The unit of cell can be represented as two cells mounted in parallel, composed of half of the base associated to emitter1 and 2. From Eq. (8) (see Fig. 3) each half of the base will act as ideal back surface field (recombination velocity at $H/2$ remained zero).

The photovoltage across the junction, according to the Boltzmann relation, is obtained as:

$$V_{Ph} = V_T\cdot\ln\left[1+\frac{Nb}{n_0^2}\cdot\delta(0)\right] \quad (10)$$

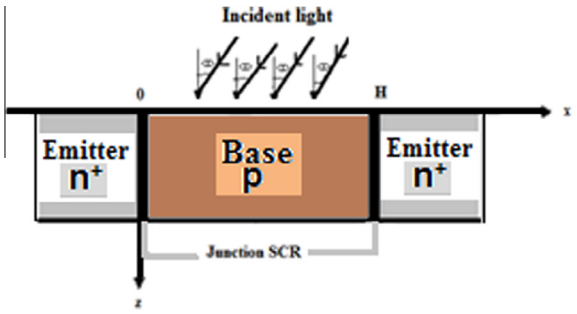

Fig. 2. Unit cell of a vertical parallel junction silicon solar cell.

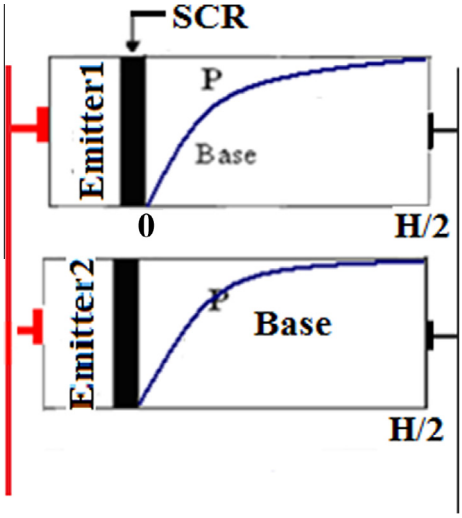

Fig. 3. Minority carrier distribution in the base.

with V_T the thermal voltage, Nb the base doping density, n_i the intrinsic carriers' density.

The series and shunt resistances are given by the relations (10) and (11) [13–19]:

$$Rs(\omega,\theta,z,Sf,\lambda) = \frac{V_{co} - V_{ph}(\omega,\theta,z,Sf,\lambda)}{J_{ph}(\omega,\theta,z,Sf,\lambda)} \quad (11)$$

$$Rsh(\omega,\theta,z,Sf,\lambda) = \frac{V_{ph}(\omega,\theta,z,Sf,\lambda)}{J_{cc} - J_{ph}(\omega,\theta,z,Sf,\lambda)} \quad (12)$$

The charge variation in the base leads to a corresponding photovoltage variation across the junction; this gives rise to an associated capacitance. This capacitance is mainly due to the fixed ionized charge (dark capacitance) at the junction boundaries and the diffusion process (diffusion capacitance) [19–26]. The solar cell's capacitance can be defined by:

$$C = \frac{dQ}{dV} \quad (13)$$

with

$$Q = q\delta(x)|_{x=0} \quad (14)$$

Given the photovoltage expression (Eq. (10), the capacitance can be rewritten as:

$$C(\omega,\theta,z,Sf,\lambda) = \frac{q}{V_T}\cdot\left(\frac{n_i^2}{Nb}+\delta(0)\right) \quad (15)$$

The conversion efficiency of the solar cell is expressed as [19,27–34]:

$$\eta(\omega,\theta,z,\lambda)=\frac{P_{max}(\omega,\theta,z,\lambda)}{P_{inc}} \quad (16)$$

P_{max} is the maximum output power for a given operating condition and P_{in} is the incident power.

Simulation results and discussion

We present in this section the simulation results obtained from all the above equations.

Series and shunt resistances

Solar cell, as simulated by essentially one-dimensional models, is assumed to show a homogeneous current flow across the whole area, both under illumination and in the dark. In the traditional interpretation of *I–V* characteristics of solar cells all nonlinear currents belonged to the cell, and only ohmic current paths across the n^+-p junction have been attributed to parasitic resistances. These parasitic resistances are the series and shunt resistances.

The profile of series resistance is shown on Figs. 4 and 5 respectively for short ($\lambda \leqslant 0.5$ μm) and long wavelengths ($\lambda > 0.5$ μm).

As can be easily seen in these figures for the long wavelengths, series resistance increases with the wavelength while for short wavelengths it is the opposite which is observed (see Figs. 4 and 5). Figs. 5 and 6 present the solar cell shunt resistance versus junction recombination velocity respectively for short ($\lambda \leqslant 0.5$ μm) and long wavelengths ($\lambda > 0.5$ μm).

Taking into account the thickness of the solar cell along *z* axis, short wavelengths generate more carriers in the base thus decreasing the dynamic resistivity of the base and thus series resistance. It is the opposite phenomenon in the long wavelength range. For the shunt resistance, we have the following profiles:

Shunt resistance always increases with the junction recombination velocity but its behavior with the wavelength depends on the considered wavelength range. In the range of short wavelengths ($\lambda \leqslant 0.5$ μm) shunt resistance decreases when the wavelength increases; for the long wavelengths ($\lambda > 0.5$ μm), it is the contrary effect which is observed. The evolution of shunt resistance with the wavelength is directly related to the absorption coefficient (penetration depth) and to the thickness of the solar cell (see Fig. 7).

We want to illustrate now the effect of illumination wavelength on the behavior of the solar cell capacitance.

Capacitance

Figs. 8 and 9 present the solar cell capacitance versus junction recombination velocity respectively for short ($\lambda \leqslant 0.5$ μm) and long wavelengths ($\lambda > 0.5$ μm).

The study of the diffusion capacitance of the solar cell depends strongly on the variation of the absorption coefficient $\alpha(\lambda)$ for a given thickness *z*. Short wavelengths are absorbed near the incident surface generating more carriers. The excess generated carriers are blocked near the junction in open circuit condition ($Sf = 0$)

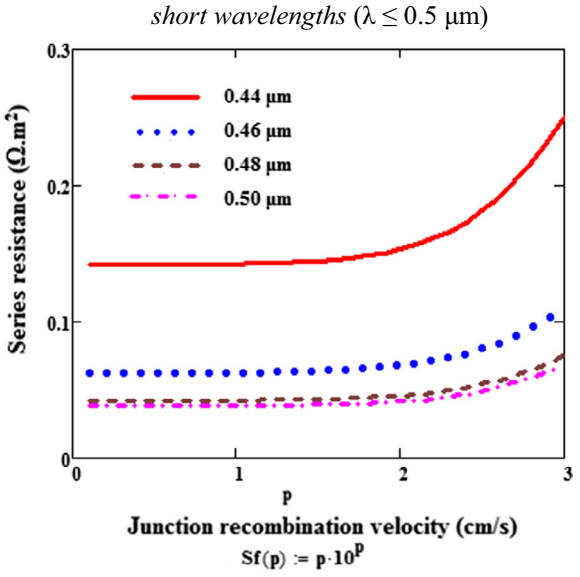

Fig. 4. Series resistance versus junction recombination velocity for various wavelengths. $L_0 = 0.0001$ cm, $D_0 = 26$ cm^2/s, $Sf = 3.10^3$ cm/s, $H = 0.03$ cm, $z = 0.0001$ cm. 1: $\lambda = 0.44$ μm; 2: $\lambda = 0.46$ μm; 3: $\lambda = 0.48$ μm; 4: $\lambda = 0.50$ μm.

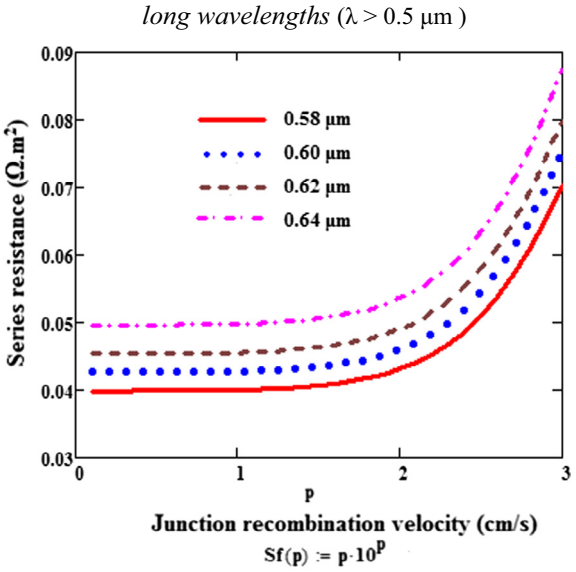

Fig. 5. Series resistance versus junction recombination velocity for various wavelengths. $L_0 = 0.0001$ cm, $D_0 = 26$ cm^2/s, $Sf = 3.10^3$ cm/s, $H = 0.03$ cm, $z = 0.0001$ cm. 1: $\lambda = 0.58$ μm; 2: $\lambda = 0.60$ μm; 3: $\lambda = 0.62$ μm; 4: $\lambda = 0.64$ μm.

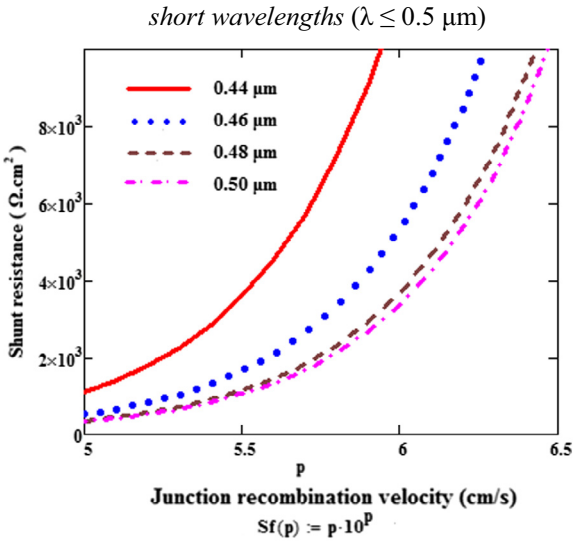

Fig. 6. Shunt resistance versus junction recombination velocity for various wavelengths. $L_0 = 0.0001$ cm, $D_0 = 26$ cm^2/s, $Sf = 3.10^3$ cm/s, $H = 0.03$ cm, $z = 0.0001$ cm. 1: $\lambda = 0.44$ μm; 2: $\lambda = 0.46$ μm; 3: $\lambda = 0.48$ μm; 4: $\lambda = 0.50$ μm.

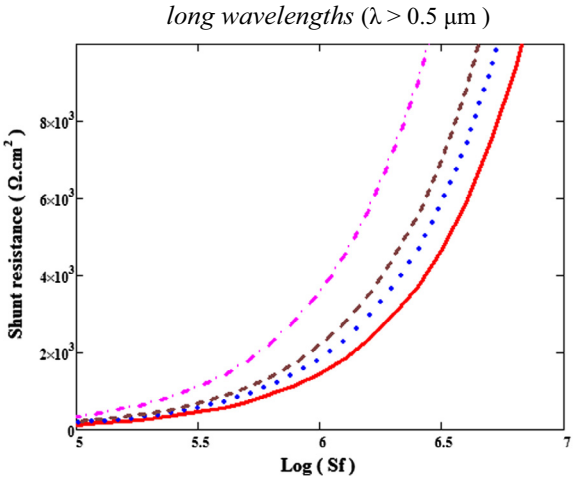

Fig. 7. Shunt resistance versus junction recombination velocity for various wavelengths. L_0 = 0.0001 cm, D_0 = 26 cm^2/s, Sf = 3.10^3 cm/s, H = 0.03 cm, z = 0.0001 cm. 1: λ = 0.58 μm; 2: λ = 0.60 μm; 3: λ = 0.62 μm; 4: λ = 0.64 μm.

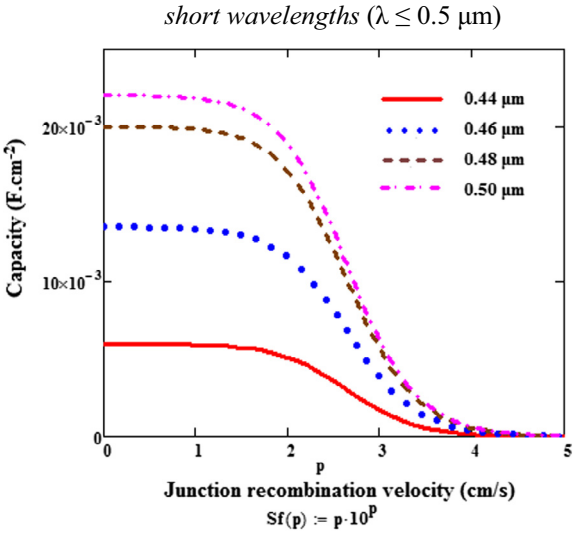

Fig. 8. Capacitance versus junction recombination velocity (logarithmic scale) for various wavelengths. L_0 = 0.0001 cm, D_0 = 26 cm^2/s, Sf = 3.10^3 cm/s, H = 0.03 cm, z = 0.0001 cm. 1: λ = 0.44 μm; 2: λ = 0.46 μm; 3: λ = 0.48 μm; 4: λ = 0.50 μm.

and give rise to large capacitance; while for short circuit condition (large Sf), the carriers flow across the junction and lead to a low value of capacitance.

With short wavelengths, we have more generation for not very thick solar cells and thus more carrier's generation; with the carrier's generation, the diffusion phenomenon takes place and the capacitance of the solar cell (mainly diffusion capacitance) increases consequently. It is the opposite phenomenon for long wavelengths.

Conversion efficiency

The conversion efficiency is the fraction of incident power converted into electric power.

The photovoltaic conversion efficiency is presented versus illumination wavelength in Fig. 10.

It makes it possible to know the effectiveness of the photovoltaic cell in the process of energy transformation.

For a given wavelength, the power depends on the photon flux. The dependence according to the wavelength is marked by the

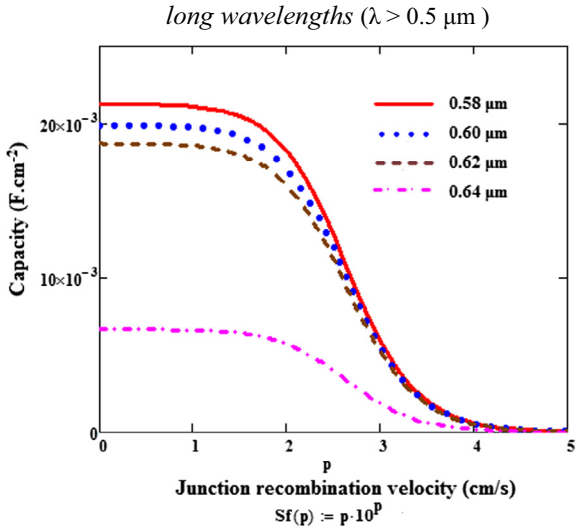

Fig. 9. Capacitance versus junction recombination velocity (logarithmic scale) for various wavelengths. L_0 = 0.0001 cm, D_0 = 26 cm^2/s, Sf = 3.10^3 cm/s, H = 0.03 cm, z = 0.0001 cm. 1: λ = 0.58 μm; 2: λ = 0.60 μm; 3: λ = 0.62 μm; 4: λ = 0.64 μm.

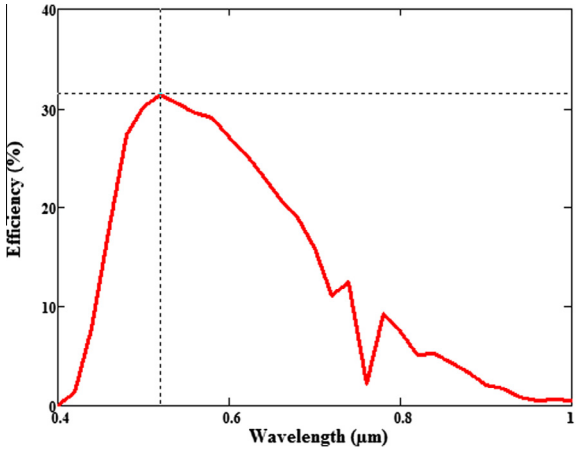

Fig. 10. Conversion efficiency versus wavelength. L_0 = 0.02 cm, D_0 = 26 cm^2/s.

considered wavelength range, as explained above: increase of the conversion efficiency with the wavelength in the case of short wavelengths and contrary effect with long wavelengths.

Conclusion

In this paper, we have developed a physical model which enables us to simulate the behavior of the vertical parallel junction solar cell. In our model, we considered only the contribution of the base. Electrical parameters such as series resistance and shunt resistances, diffusion capacitance and the photovoltaic conversion efficiency were then determined and computed versus the junction recombination velocity, for various wavelengths.

Our computed results have shown that the performance of solar cell is better in the short wavelengths range and conversion efficiency reaches about 32%.

References

[1] Orton JW, Blood P. The Electrical characterization of semiconductors: measurement of minority carrier properties. London: Academic Press; 1990.
[2] Zondervan A, Verhoef LA, Lindholm FA. Measurement circuits for silicon-diode and solar-cell lifetime and surface recombination velocity by electrical short-circuit current decay. IEEE Trans Electron Dev 1988;Ed-35:85–8.

[3] Ray UC, Agarwal SK. Wavelength dependence of short- circuit current decay in solar cells. J Appl Phys 1988;63:547–9.
[4] Sissoko G, Museruka C, Corréa A, Gaye I, Ndiaye AL. Light spectral effect on recombination parameters of silicon solar cell. World Renewable Energy Congress, Part III 1996:1487–90.
[5] Honma Noriaki, Munakata Chusuke. Sample thickness dependence of minority carrier lifetimes measured using an ac photovoltaic method. Jpn J Appl Phys 1987;26(12):233–6.
[6] Noriaki Honma, Chusuke Munakata, Hirofimi Shimizu. Calibration of minority carrier lifetimes measured with an ac photovoltaic method. Jpn J Appl Phys july 1988;27(7):1322–6.
[7] Mandelis Andreas. Coupled ac photocurrent and photothermal reflectance response theory of semiconducting p-n junctions. J Appl Phys 1989;66 (11):5572–83.
[8] Dieng A, Zerbo I, Wade M, Maiga AS, Sissoko G. Three-dimensional study of a polycrystalline silicon solar cell: the influence of the applied magnetic field on the electrical parameters. Semicond. Sci. Technol. 2011;26. 095023 (9pp).
[9] Diallo HL, Wereme A, Maiga AS, Sissoko G. New approach of both junction and back surface recombination velocities in a 3D modelling study of a polycrystalline silicon solar cell. Eur Phys J Appl Phys 2008;42:203–11.
[10] Gover Avraham, Stella Paul. Vertical multijunction solar-cell one-dimensional analysis. IEEE Trans Electron Devices 1974;ed-21(6):351–6.
[11] Ndiaye El Hadji, Sahin Gokhan, Dieng Moustapha, Thiam Amary, Diallo Hawa Ly, Ndiaye Mor, Sissoko Grégoire. Study of the intrinsic recombination velocity at the junction of silicon solar under frequency modulation and irradiation. J Appl Math Phys 2015;3:1522–35. http://dx.doi.org/10.4236/jamp.2015.311177. Published Online November 2015 in SciRes. http://www.scirp.org/journal/jamp,.
[12] Bashahu M, Habyarimana A. Review and test of methods for determination of the solar cell series resistance. Renewable Energy 1995;6(2):127–38.
[13] Diallo HL, Dieng B, Ly I, Dione MM, Ndiaye M, Lemrabott OH, Bako ZN, Wereme A, Sissoko G. Determination of the recombination and electrical parameters of a vertical multijunction silicon solar cell. Res J Appl Sci Eng Technol 2012;4 (16):2626–31.
[14] Pysch D, Mette A, Glunz SW. A review and comparison of different methods to determine the series resistance of solar cells. Sol Energy Mater Sol Cells 2007;91:1698–706.
[15] El- Adawi MK, Al- Nuaim IA. A method to determine the solar cell series resistances from a single I-V characteristic curve considering its shunt resistance-new approach. Vaccum 2002;64:33–6.
[16] Mbodji S, Ly I, Diallo HL, Dione MM, Diasse O, Sissoko G. Modeling study of n+/p solar cell resistances from single I-V characteristic curve considering the junction recombination velocity (Sf). Res J Appl Sci Eng Technol 2012;4(1):1–7.
[17] Barro Fabe Idrissa, Sane Moustapha, Zouma Bernard. On the capacitance of crystalline silicon solar cells in steady state. Turk J Phys 2015;39:122–7. http://dx.doi.org/10.3906/z-1408-3. TUBITAK.
[18] Balenzategui JL, Chenlo F. Measurement and analysis of angular response of bare and encapsulated silicon solar cells. Sol Energy Mater Sol Cells 2005;86:53–83.
[19] Wenham SR, Green MA, Watt ME, Corkish R. Applied Photovoltaics. 2nd ed. ARC Centre for Advanced Silicon Photovoltaics and Photonics; 2007.
[20] Hu CC. Modern semiconductor devices for integrated circuits. New Jersey: Pearson/Prentice Hall; 2010.
[21] Colinge JP, Colinge CA. Physics of semiconductor devices. Kluwer Academic Publishers; 2002.
[22] Neamen DA. Semiconductor physics and devices: basic principles. 3rd Ed. McGraw-Hill; 2003.
[23] H. Mathieu et H. Fanet, "Physique des semiconducteurs et des composants électroniques", 6ème Ed, Dunod; 2009.
[24] Boer KW. Introduction to space charge effects in semiconductor. Springer-Verlag; 2010.
[25] B. Van Zeghbroeck, Principles of Semiconductor Devices; 2011.
[26] Sane Moustapha, Sahin Gokhan, Barro Fabe drissa, Maiga Amadou Seidou. Incidence angle and spectral effects on vertical junction silicon solar cell capacitance. Turk J Phys 2014;38:221–7. http://dx.doi.org/10.3906/fiz-1311-9. TUBITAK.
[27] Sahin Gokhan, Dieng Moustapha, El Moujtaba Mohamed Abderrahim Ould, Ngom Moussa Ibra, Thiam Amary, Sissoko Grégoire. Capacitance of vertical parallel junction silicon solar cell under monochromatic modulated illumination. J Appl Math Phys 2015;3:1536–43. http://dx.doi.org/10.4236/jamp.2015.311178. Published Online November 2015 in SciRes. http://www.scirp.org/journal/jamp.
[28] Wenham SR, Green MA, Watt ME, Corkish R. Applied Photovoltaics. 2nd ed. ARC, Centre for Advanced Silicon Photovoltaics and Photonics; 2007.
[29] "World record solar cell with 44.7% efficiency". Science Daily. Retrieved 2014–06-22.
[30] Jump up, De Vos A, Pauwels H. On the thermodynamic limit of photovoltaic energy conversion. Appl Phys 1981;25:119–25. http://dx.doi.org/10.1007/BF00901283. Bibcode:1981ApPhy. 25...119D.
[31] Jump up, Cheng-Hsiao Wu, Williams Richard. Limiting efficiencies for multiple energy-gap quantum devices. J Appl Phys 1983;54:6721. http://dx.doi.org/10.1063/1.331859. Bibcode:1983JAP....54.6721W.
[32] Jump up, Molki A. Dust affects solar-cell efficiency. Phys Educ 2010;45:456–8. http://dx.doi.org/10.1088/0031-9120/45/5/F03. Bibcode:2010PhyEd.45.456M.
[33] Jump up, Nelson Jenny. The Physics of Solar Cells. Imperial College Press; 2003. ISBN 978-1-86094-340-9.
[34] Jump up, "Solar Junction Breaks Its Own CPV Conversion Efficiency Record". 2013-12-18. Retrieved 2013-12-18.